Isomeric C_{12}-Alkamides from the Roots of *Echinacea purpurea* Improve Basal and Insulin-Dependent Glucose Uptake in 3T3-L1 Adipocytes

Authors Dorota Kotowska[1]*, Rime B. El-Houri[2]*, Kamil Borkowski[1], Rasmus K. Petersen[1], Xavier C. Fretté[2], Gerhard Wolber[3], Kai Grevsen[4], Kathrine B. Christensen[2], Lars P. Christensen[2], Karsten Kristiansen[1]

Affiliations The affiliations are listed at the end of the article

Key words
- *Echinacea purpurea*
- Asteraceae
- alkamides
- adipocytes
- glucose uptake
- PPARγ partial agonist

received June 24, 2014
revised August 23, 2014
accepted October 12, 2014

Bibliography
DOI http://dx.doi.org/10.1055/s-0034-1383252
Published online November 5, 2014
Planta Med 2014; 80: 1712–1720 © Georg Thieme Verlag KG Stuttgart · New York · ISSN 0032-0943

Correspondence
Prof. Dr. Lars P. Christensen
Department of Chemical Engineering
Biotechnology and Environmental Technology
University of Southern Denmark
Campusvej 55
5230 Odense M
Denmark
Phone: + 45 65 50 73 61
Fax: + 45 65 50 73 54
lpc@kbm.sdu.dk

Abstract

Echinacea purpurea has been used in traditional medicine as a remedy for the treatment and prevention of upper respiratory tract infections and the common cold. Recent investigations have indicated that *E. purpurea* also has an effect on insulin resistance. A dichloromethane extract of *E. purpurea* roots was found to enhance glucose uptake in adipocytes and to activate peroxisome proliferator-activated receptor γ. The purpose of the present study was to identify the bioactive compounds responsible for the potential antidiabetic effect of the dichloromethane extract using a bioassay-guided fractionation approach. Basal and insulin-dependent glucose uptake in 3T3-L1 adipocytes were used to assess the bioactivity of extract, fractions and isolated metabolites. A peroxisome proliferator-activated receptor γ transactivation assay was used to determine the peroxisome proliferator-activated receptor γ activating properties of the extract, active fractions and isolated metabolites. Two novel isomeric dodeca-2*E*,4*E*,8*Z*,10*E*/*Z*-tetraenoic acid 2-methylbutylamides together with two known C_{12}-alkamides and α-linolenic acid were isolated from the active fractions. The isomeric C_{12}-alkamides were found to activate peroxisome proliferator-activated receptor γ, to increase basal and insulin-dependent glucose uptake in adipocytes in a dose-dependent manner, and to exhibit characteristics of a peroxisome proliferator-activated receptor γ partial agonist.

Abbreviations

aP2:	adipocyte protein 2
C/EBPα:	CCAAT/enhancer-binding protein α
CS:	calf serum
DCM:	dichloromethane
DI:	dexamethasone and insulin
DMEM:	Dulbecco's modified Eagle's medium
FCS:	fetal calf serum
Glut:	glucose transporter
GST:	glutathionine-*S*-transferase
GU:	glucose uptake
LBD:	ligand binding domain
MDI:	1-methyl-3-isobutylxanthine, dexamethasone and insulin
PBS:	phosphate-buffered saline
PPAR:	peroxisome proliferator-activated receptor
qPCR:	real-time quantitative polymerase chain reaction
Rosi:	rosiglitazone
SCD1:	stearoyl-coenzyme A desaturase 1
T2D:	type 2 diabetes
TFA:	trifluoroacetic acid
TR-FRET:	time-resolved fluorescence resonance energy transfer
TZD:	thiazolidinedione

Supporting information available online at http://www.thieme-connect.de/products

Introduction

Echinacea purpurea (L.) Moench. (Asteraceae) is commonly used in traditional medicine for the treatment and prevention of upper respiratory tract infections and the common cold. Commercial medicinal preparations of *E. purpurea* have been shown to possess immunomodulatory and anti-inflammatory effects which explain the traditional use of the plant [1,2]. Furthermore, we have previously shown that lipophilic extracts of

* Dorota Kotowska and Rime B. El-Houri contributed equally to the work.

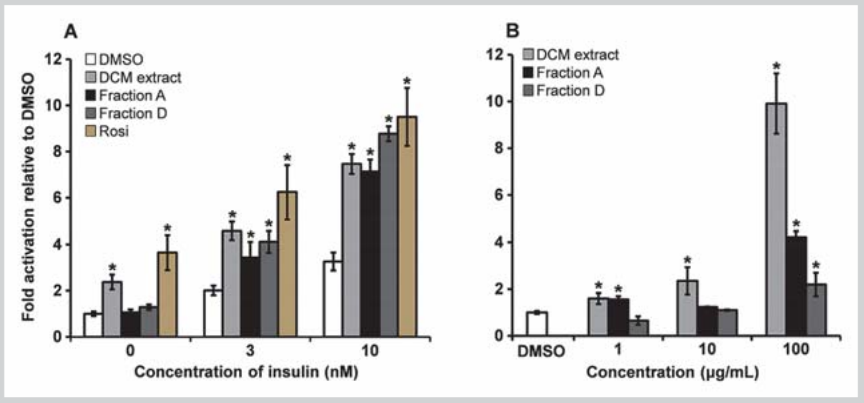

Fig. 1 Effects of dichloromethane extract of *Echinacea purpurea* roots and active fractions A and D on: **A** Glucose uptake in adipocytes at 100 µg/mL with insulin concentrations of 0, 3, and 10 nM. **B** PPARγ transactivation at 1, 10, and 100 µg/mL. DMSO (vehicle) was set to 1 and the results normalized to this, while Rosi (1 µM) was the positive control. In the PPARγ transactivation assay, Rosi was 37-fold relative to DMSO. All values are expressed as mean ± SD of three independent experiments in triplicates; * $p < 0.001$ indicates significance relative to DMSO. (Color figure available online only.)

E. purpurea activate PPARγ and enhance insulin-stimulated GU in adipocytes *in vitro* in a dose-dependent manner [3,4] and thus may have an effect on insulin resistance and T2D.

Adipose tissue plays a key role in energy homeostasis as a metabolic and endocrine organ. Adipocytes are targets for drugs reducing obesity or ameliorating obesity-associated metabolic disorders such as T2D [5]. TZDs have been used as insulin sensitizers in the management of T2D. TZDs regulate the expression of genes involved in insulin signaling and glucose and lipid metabolism in mature adipocytes but also promote adipocyte differentiation by acting as PPARγ full agonists setting into motion gene cascades promoting differentiation and accumulation of triglycerides in adipocytes accentuating adiposity [6]. Furthermore, the potent TZDs cause undesirable side effects, including edema, fluid retention, weight gain, cardiac failure, and hepatotoxicity. Due to the observed hepatotoxicity, two TZD drugs were recently withdrawn from the market and the remaining one, pioglitazone, has been reassessed in light of increased risk of bladder cancer [7]. Limitations of the TZDs have driven research towards new types of drugs, which are able to increase insulin sensitivity acting as PPARγ partial agonists, and therefore possibly ameliorate obesity-related insulin resistance without causing the side effects observed in relation to many, if not all, full PPARγ agonists.

A number of natural plant-derived compounds have been shown to improve insulin sensitivity and may thus serve as starting point for discovery and design of novel drugs and herbal medicine to treat and prevent metabolic disorders with fewer side effects compared to synthetic drugs [8]. The bioactive metabolites considered responsible for the pharmacological activities of *E. purpurea* comprise polysaccharides, caffeic acid derivatives and alkamides [1,4,9–11]. From the florets of *E. purpurea*, a C_{16}-alkamide has been isolated that significantly activated PPARγ and stimulated GU in adipocytes *in vitro* [4]. The roots of *E. purpurea* have a relative high content of alkamides [12–14], of which some are known for their immunomodulatory and anti-inflammatory effects [1,2]. However, very little is known about these bioactive compounds in relation to their effects on GU and PPARγ. In the present study, it is shown that a crude DCM extract of *E. purpurea* roots was able to enhance GU in 3T3-L1 adipocytes and to activate PPARγ. Hence, we decided to identify the metabolites responsible for the potential antidiabetic effect of this lipophilic extract using a bioassay-guided fractionation approach. Basal and insulin-dependent GU in adipocytes were used to assess the bioactivity of fractions and isolated compounds. In addition, we determined the PPARγ activating properties of active fractions and isolated metabolites in order to determine how their effect on GU in adipocytes correlated with their PPARγ activating properties.

Results and Discussion

We have previously screened 133 plant extracts in different assays including PPARγ transactivation, adipocyte differentiation, and insulin-dependent GU [3]. In this former investigation, the crude DCM root extract of *E. purpurea* was found to activate PPARγ and to increase insulin-dependent GU, while it did not promote adipogenesis. The present study stays in agreement with these data (**Fig. 1**; **Fig. 1S**, Supporting Information). The results revealed that basal GU in cells treated with the DCM extract was increased approximately 2-fold compared to control and was enhanced in the presence of 3 and 10 nM of insulin, suggesting that the extract increased insulin sensitivity in 3T3-L1 adipocytes (**Fig. 1A**). Furthermore, the DCM extract was shown to activate PPARγ in transfected cell cultures in a dose-dependent manner (**Fig. 1B**), acting as a weak PPARγ agonist compared to the full agonist Rosi, and did not inhibit MDI-induced adipocyte differentiation or promote adipocyte differentiation of DI-treated 3T3-L1 preadipocytes (**Fig. 1S**).

A bioassay-guided approach was used to identify active metabolites from the crude DCM extract with interesting properties in relation to GU. Initial separation of the extract by flash chromatography resulted in nine fractions (A–I), of which fractions A and D were found to increase insulin-dependent GU in the presence of 3 nM and 10 nM insulin (**Fig. 1A**). The observed effect of the active fractions A and D on GU could be due to the presence of natural products with PPARγ activity, and they were therefore tested for this activity. Fractions A and D were found to activate PPARγ acting as weak agonists (**Fig. 1B**). However, the lack of correlation between insulin-dependent GU and PPARγ activity (**Fig. 1**) suggests that the effect on GU uptake, at least partially, may be due to compounds acting as partial agonists. In addition, fractions A and D did not promote adipogenesis using the DI protocol (**Fig. 1S**, Supporting Information).

HPLC-PDA-APCI-MS/MS analysis revealed that fraction A contained fatty acids with α-linolenic acid being a major constituent, while fraction D contained alkamides. α-Linolenic acid is a well-known PPARγ agonist [4,15] and has previously been shown to improve glucose tolerance, insulin sensitivity, dyslipidemia, hypertension, and ventricular stiffness in rats [16,17]; thus fraction A was not investigated further. Separation of fraction D by semi-preparative HPLC yielded four alkamides (**Fig. 2A**), of which

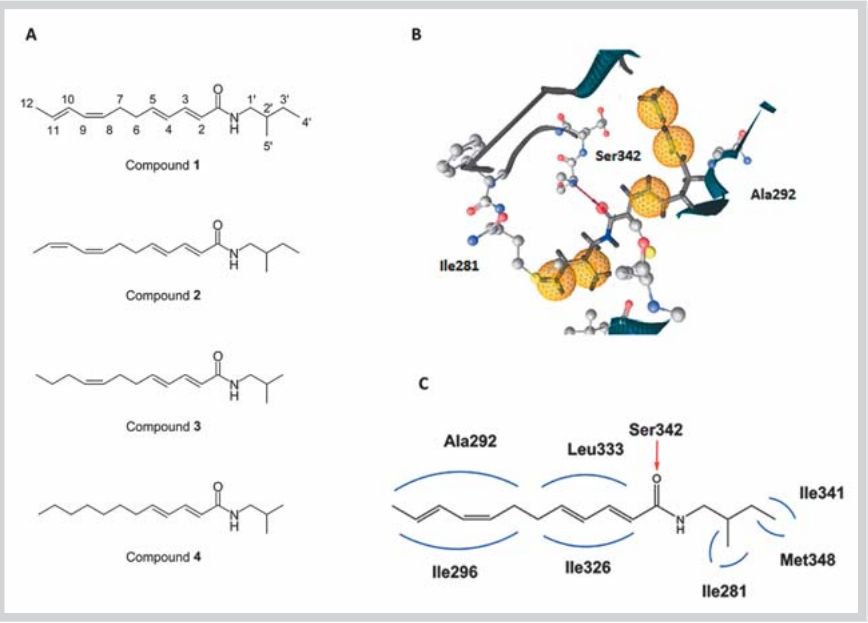

Fig. 2 **A** Chemical structures of alkamides (compounds **1**–**4**) isolated from an active fraction (fraction D) of a dichloromethane root extract of *Echinacea purpurea*. Compounds **1** and **2** were isolated as an inseparable mixture (named compounds **1**/**2**). **B** Predicted binding modes of compounds **1**/**2** shown as a 3D representation. **C** 2D representation of the chemical features of the interaction pattern derived from the docking pose for compound **1**. The interaction pattern is the same for compound **2**. Chemical features in the 2D representation are: red arrow = hydrogen-bond donor; blue line = hydrophobic contacts.
(Color figure available online only.)

two are new isomeric C_{12}-alkamides (**1, 2**). The known alkamides dodeca-2*E*,4*E*,8*Z*-trienoic acid isobutylamide (**3**) and dodeca-2*E*,4*E*-dienoic acid isobutylamide (**4**) have previously been isolated from the roots of *E. purpurea* [12, 14, 18].

Compounds **1** and **2** were obtained as an inseparable 1 : 1 mixture (compounds **1**/**2**) that gave a quasi-molecular precursor ion at *m/z* 262 $[M + H]^+$. The molecular formula $C_{17}H_{27}NO$ (5 degrees of unsaturation) was assigned based on HR-ESI-MS data. The MS/MS fragmentation pattern of the quasi-molecular precursor ion of compounds **1**/**2** showed characteristic product ions for 2-methylbutylamides (**Fig. 3**) [13, 14, 19–21]. The presence of a 2-methylbutylamine moiety was confirmed by the ^{1}H NMR signals at δ 0.90 (d, J = 7 Hz, H_3-5′), 0.90 (t, J = 7 Hz, H_3-4′), 1.17 (m, H-3′b), 1.41 (m, H-3′a), 1.58 (m, H-2′), 3.16 (m, H-1′b), 3.28 (m, H-1′a), and 5.43 (brs, NH) [12], and was further substantiated by the ^{1}H–^{1}H COSY spectrum (**Table 1**). The UV spectrum showed absorption maxima at 235 and 261 nm indicating a 2,4-diene moiety and an additional diene chromophore in the structure of **1** and **2** [12, 21]. The relative intensities of the fragments at *m/z* 149 (100%, base peak) and *m/z* 147 (24%) of the MS/MS fragmentation pattern were in agreement with compounds **1**/**2** being 2,4-diene alkamides [13, 14, 20]. The presence of four carbon-carbon double bonds in **1** and **2** was evident from the ^{1}H NMR showing signals from 2 × 8 olefinic protons (**Table 1**). The low-field shift of the methine proton at C-3 (δ 7.18) confirmed that one of the double bonds was attached next to the amide moiety [12, 22]. The positions of the other double bonds were determined from the ^{1}H–^{1}H COSY spectrum thus establishing the four double bonds in positions 2, 4, 8, and 10, respectively (**Table 1**). The double bonds in positions 2 and 4 were assigned an *E* configuration on the basis of a coupling constant of 15 Hz, and the double bond in position 8 was assigned a *Z* configuration due to a coupling constant of 11 Hz [12]. Similarly, the double bond in position 10 was assigned as being *E* or *Z* (**Table 1**). Hence, the chemical structure of compounds **1** and **2** was established as dodeca-2*E*,4*E*,8*Z*,10*E*-tetraenoic acid 2-methylbutylamide and dodeca-2*E*,4*E*,8*Z*,10*Z*-tetraenoic acid 2-methylbutylamide, respectively (**Fig. 2A**).

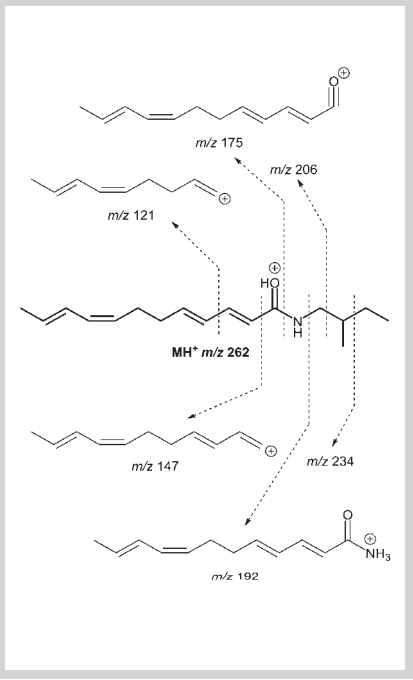

Fig. 3 Proposed fragmentation pathway of the protonated molecular ion (MH^+) of dodeca-2*E*,4*E*,8*Z*,10*E*-tetraenoic acid 2-methylbutylamide (**1**) as determined by MS/MS, including chemical structures of some of the most characteristic fragments. The base peak fragment at *m/z* 149 (not shown) is probably formed when a double bond of the original 2,4-diene shifts to the 3-position, with a subsequent gain of two hydrogens [13, 14, 20]. The fragmentation pathway of the 2*E*,4*E*,8*Z*,10*Z*-isomer (**2**) is the same as illustrated above.

Compounds **3** and **4** showed a weak increase of basal GU and insulin-dependet GU at 3 nM insulin in mature 3T3-L1 cells at 30 µM, whereas no increase of insulin-dependent GU was observed at 10, 30 and 100 nM insulin (**Fig. 2S**, Supporting Information) despite their ability to weakly activate PPARγ, which is, for compound **4**, in accordance with previous investigations [4]. Dodeca-2*E*,4*E*,8*Z*,10*E*/*Z*-tetraenoic acid isobutylamides are among the major alkamides in *E. purpurea* but have previously been shown not to activate PPARγ [4]. This may also explain why these alkamides were detected in the non-active fraction F according to the GU bioassay (data not shown). Compounds **1**/**2** at 30 µM significantly increased basal GU 6.3-fold compared to the vehicle and 3-fold compared to Rosi (**Fig. 4A**). A significant stimulation of insulin-dependent GU in the presence of 3, 10, 30 and 100 nM

H	Compound 1	Compound 2	^{1}H–^{1}H COSY correlations
	δ ^{1}H (ppm) (*J* in Hz)	δ ^{1}H (ppm) (*J* in Hz)	
2	5.76 d (15 Hz)	5.76 d (15 Hz)	H-3
3	7.18 dd (15; 11 Hz)	7.18 dd (15; 11 Hz)	H-2, H-4
4	6.17 dd (15; 11 Hz)	6.17 dd (15; 11 Hz)	H-3, H-5
5	6.08 dt (15; 7 Hz)	6.08 dt (15; 7 Hz)	H-4, H_2-6
6	2.28 m	2.28 m	H-5, H_2-7
7	2.28 m	2.28 m	H_2-6, H-8
8	5.25 m	5.36 m	H_2-7, H-9
9	5.97 dd (11; 11 Hz)	6.30 dd (11; 11 Hz)	H-8, H-10
10	6.25 dd (15; 11 Hz)	6.32 dd (11; 11 Hz)	H-9, H-11
11	5.69 dq (15; 7 Hz)	5.55 dq (11; 7 Hz)	H-10, H_3-12
12	1.78 brd (7 Hz)	1.75 brd (7 Hz)	H-11
NH	5.43 brs	5.43 brs	H_2-1′
1′a	3.28 m	3.28 m	H-2′, NH
1′b	3.16 m	3.16 m	H-2′, NH
2′	1.58 m	1.58 m	H_2-1′, H_2-3′, H_3-5′
3′a	1.41 m	1.41 m	H-2′, H_3-4′
3′b	1.17 m	1.17 m	H-2′, H_3-4′
4′	0.90 t (7 Hz)	0.90 t (7 Hz)	H_2-3′
5′	0.90 d (7 Hz)	0.90 d (7 Hz)	H-2′

Table 1 ^{1}H NMR and ^{1}H–^{1}H COSY spectral data ($CDCl_3$, 400 MHz) of dodeca-2*E*,4*E*,8*Z*,10*E*-tetraenoic acid 2-methylbutylamide (**1**) and dodeca-2*E*,4*E*,8*Z*,10*Z*-tetraenoic acid 2-methylbutylamide (**2**).

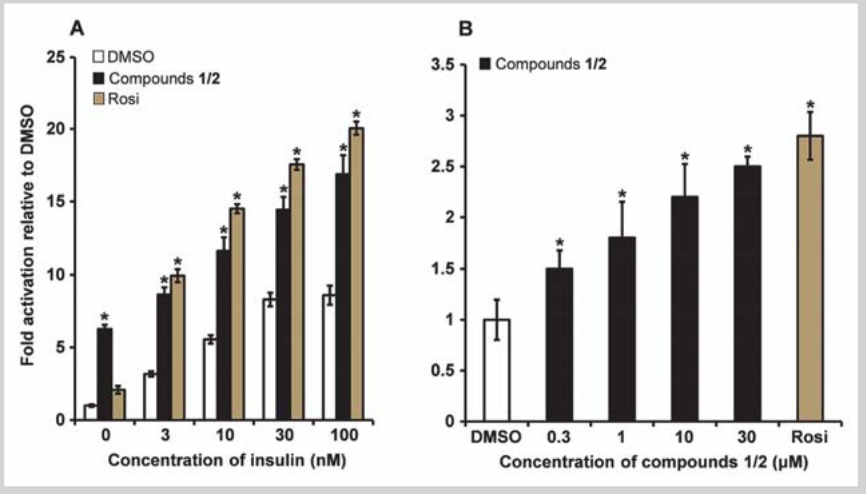

Fig. 4 Effect of compounds **1**/**2** on insulin-dependent glucose uptake: **A** At 30 µM of compounds **1**/**2** with insulin concentrations of 0, 3, 10, 30 and 100 nM. **B** Dose-dependent effect of compounds **1**/**2** at 10 nM insulin. DMSO (vehicle) was set to 1 and the results normalized to this, while Rosi (1 µM) was the positive control. All values are expressed as mean ± SD of three independent experiments in triplicates; * $p < 0.001$ indicates significance relative to DMSO. (Color figure available online only.)

insulin was also observed in cells treated with 30 µM of compounds **1**/**2** (**Fig. 4A**). Compounds **1**/**2** also dose-dependently increased GU in the presence of 10 nM insulin (**Fig. 4B**). The effects of compounds **1**/**2** on GU resemble those of hexadeca-2*E*,9*Z*,12*Z*,14*E*-tetraenoic acid isobutylamide, previously isolated from the flowers of *E. purpurea* [4]. Similar to hexadeca-2*E*,9*Z*,12*Z*,14*E*-tetraenoic acid isobutylamide, compounds **1**/**2** increased transactivation of PPARγ significantly at a concentration of 30 µM compared to vehicle but still weak relative to Rosi (**Fig. 5A**). Furthermore, compounds **1**/**2** and Rosi both competed with a fluorescent pan PPAR agonist in a ligand binding assay indicating a common binding site in the PPARγ LBD (**Fig. 5B**) [23]. These results indicate that compounds **1**/**2** may function as PPARγ partial agonists. The docking mode and interactions of compounds **1**/**2** with the LBD (**Fig. 2B, C**) support the assumption that compounds **1**/**2** are PPARγ partial agonists. The PPARγ LBD contains a large Y-shaped ligand binding cavity consisting of an entrance (arm III) that branches off into two binding pockets (arm I and II). Arm I is the only substantially polar cavity of the PPARγ LBD, whereas arms II and III are mainly hydrophobic [24, 25]. The predicted binding modes of compounds **1**/**2** with the PPARγ LBD included one hydrogen bond with Ser342 and several hydrophobic contacts with Ala292, Ile281, Ile296, Ile326, Ile341, Leu333, and Met348 from arms II and III of the LBD of PPARγ (**Fig. 2C**). These contacts are typical for PPARγ partial agonists [24]. The fact that dodeca-2*E*,4*E*,8*Z*,10*E*/*Z*-tetraenoic acid isobutylamides do not seem to activate PPARγ suggests that the hydrophobic contacts to Ile341 and Met348 are important for compounds **1**/**2** being PPARγ partial agonists. In addition, no hydrogen bond interaction between **1**/**2** and residues Ser289, His323, His449, and/or Tyr473 from arm I of the LBD of PPARγ was predicted, which are typical for PPARγ full agonists. It has been a general notion that the binding mode of PPARγ partial agonists affects the recruitment of co-activators differently from that of full agonists and decreases the transactivation activity of PPARγ resulting in fewer side effects, but still maintains an insulin sensitizing effect [26]. In the present study, the weak activation of PPARγ by compounds **1**/**2**, combined with the results of the competitive PPARγ binding assay and the docking mode of **1**/**2**, suggests that these compounds are acting as PPARγ partial agonists and that the 2-methylbutylamide moiety is important for their activity.

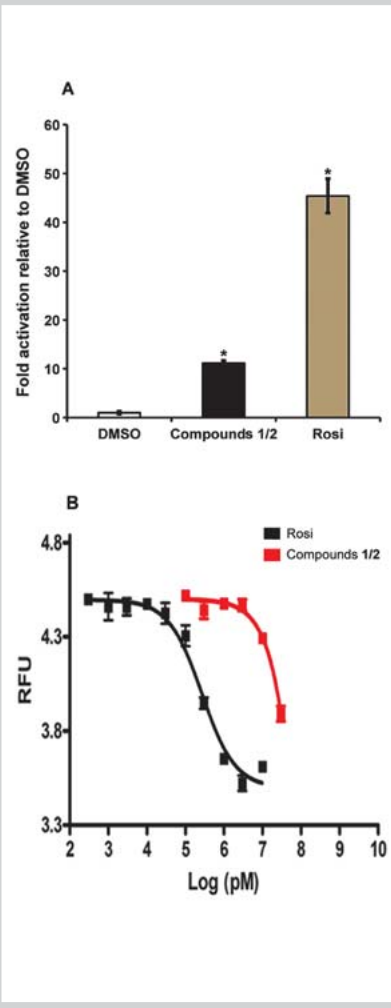

Fig. 5 Effect of compounds **1**/**2** on peroxisome proliferator-activated receptor γ: **A** Transactivation of PPARγ at a concentration of 30 µM. DMSO (vehicle) was set to 1 and the results normalized to this. Rosi (1 µM) was the positive control. All values are expressed as mean ± SD of three independent experiments in triplicates; * $p < 0.001$ indicates significance relative to DMSO. **B** Effect of Rosi (0.001–3 µM) and compounds **1**/**2** (0.1, 0.3, 1, 3, 10, and 30 µM) in LanthaScreen™ TR-FRET competitive PPARγ binding assay in the agonist mode. Relative fluorescence units (RFU) are expressed as mean ± SD of three independent experiments in triplicates. An unrestrained sigmoidal (one-binding site) dose-response curve was fitted to each data set by linear regression. (Color figure available online only.)

The alkamides are structurally related to natural endogenous and/or dietary PPARγ ligands such as fatty acids [27,28], prostanoids [28,29], phospholipids [30], and polyacetylenes [31]. The PPARγ activating properties of these ligands depend on the length of their aliphatic chain and functional groups such as carboxylate/carboxyl, α,β-unsaturated ketone, and/or hydroxyl, and thus on their interactions with the LBD. For example, the PPARγ activating properties of some endogenous prostanoids and oxidized polyunsaturated fatty acids seem to be related to their ability to bind covalently to Cys285 of PPARγ LBD through a Michael addition reaction with an α,β-unsaturated ketone [32–34]. Polyacetylenes of the falcarindiol-type containing hydroxyl groups at one or two positions along their C_{17}-aliphatic chain were also shown to display PPARγ partial agonism, which was confirmed by molecular docking studies suggesting a binding to the LBD in a manner similar to that observed for compounds **1**/**2** and other PPARγ partial agonists [31]. However, the large cavity of the PPARγ LBD, and thus the broad specificity of this receptor, makes the prediction of PPARγ activity of ligands such as alkamides and other fatty acid derivatives difficult based on their chemical structure alone, in accordance with the results of the present study.

Increased expression of adipose cell differentiation markers is associated with insulin sensitivity [35], which may to some extent explain the insulin-dependent and basal GU data obtained in this study. The critical window for ligand-dependent induction of adipocyte differentiation of 3T3-L1 preadipocytes is days 0 to 4 after induction of differentiation [36]. To investigate possible mechanisms by which compounds **1**/**2** might affect the early stages of adipocyte differentiation, we examined the expression of genes involved in adipogenesis (PPARγ, C/EBPα, and aP2, also known as fatty acid binding protein 4), glucose transport (Glut1 and Glut4), lipogenesis (SCD1), and adipokine (adiponectin) (**Table 2**) in mature 3T3-L1 cells treated with 30 µM of compounds **1**/**2** during the first 4 days of differentiation (days 0–4) using the DI and MDI protocols. Compounds **1**/**2** increased the expression of PPARγ, aP2, C/EBPα, adiponectin and Glut1 in the MDI differentiation medium (**Fig. 6A**). However, when the cAMP elevating agent 1-methyl-3-isobutylxanthine was omitted in the cocktail (DI differentiation medium), the expression of several genes was significantly downregulated (**Fig. 6B**). These results suggest that compounds **1**/**2** require elevated cAMP levels to increase the expression of key markers of adipogenesis. SCD1 expression was significantly downregulated by treatment with 30 µM of compounds **1**/**2** in both the MDI and DI treatment (**Fig. 6**). SCD1 is involved in lipogenesis, and therefore a downregulation of this gene may result in decreased lipogenesis and a small size of lipid droplets [37].

PPARγ agonists are known to increase glucose transport and insulin sensitivity by regulating expression of several genes involved in glucose metabolism [38]. GU in adipocytes is correlated with the number of glucose transporters [39]. Glut1 is expressed in both preadipocytes and mature adipocytes and is responsible for basal glucose transport. By contrast, Glut4 is expressed only in mature adipocytes and supports insulin-dependent GU [40,41]. In this study, compounds **1**/**2** increased gene expression of Glut1,

Table 2 Primer sequences used for analysis of gene expression.

Genes	5′-prime (forward)	3′-prime (reverse)
Adipogenesis process related		
C/EBPα	CAAGAACAGCAACGAGTACCG	GTCACTGGTCAACTCCAGCAC
aP2	CTGGGCGTGGAATTCGAT	GCTCTTCACCTTCCTGTCGTCT
PPARγ	ACAGCAAATCTCTGTTTTATGC	TGCTGGAGAAATCAACTGTGG
Adipokine gene		
Adiponectin	GATGGCAGAGATGGCACTCC	CTTGCCAGTGCTGCCGTCAT
Glucose transporter		
Glut1	TGTATCCTGTTGCCCTTCTGC	CGACCCTCTTCTTTCATCTCCT
Glut4	CAGAAGGTGATTGAACAGAGC	CCCTGATGTTAGCCCTGAG
Lipogenesis related		
SCD1	ACACCTGCCTCTTCGGGATT	TGATGGCCAGAGCGCTG
Reference gene		
TATA box-binding protein	ACCCTTCACCAATGACTCCTATG	ATGATGACTGCAGCAAATCGC

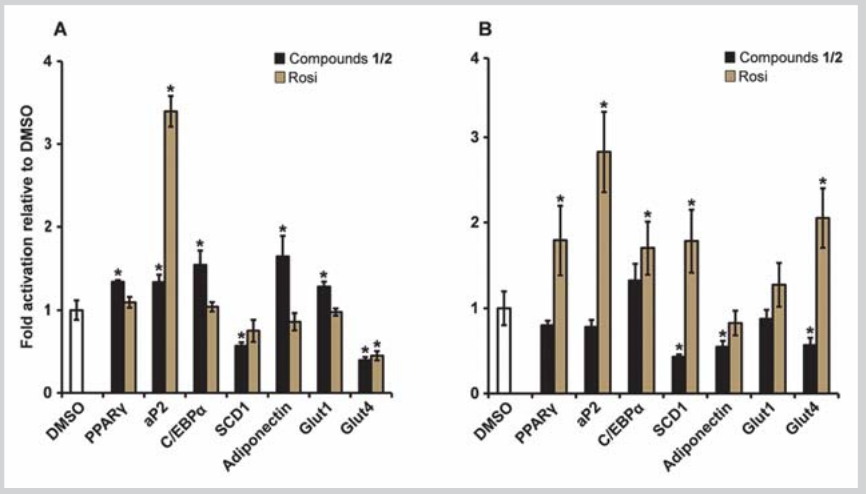

Fig. 6 Effect of compounds **1**/**2** in a concentration of 30 µM on gene expression of peroxisome proliferator-activated receptor γ, adipocyte protein 2, CCAAT/enhancer-binding protein α, stearoyl-coenzyme A desaturase 1, adiponectin, glucose transporters 1 and 4 in differentiating 3T3-L1 cells in the: **A** MDI protocol. **B** DI protocol. DMSO (vehicle) was set to 1 and the results normalized to this, while Rosi (1 µM) was the positive control. All values are expressed as mean ± SD of three independent experiments in triplicates; * $p < 0.001$ indicates significance relative to DMSO. (Color figure available online only.)

but not Glut4, when the MDI differentiation medium was used (**Fig. 6A**), whereas compounds **1**/**2** decreased the expression of the Glut4 transporter and did not significantly affect the expression of the Glut1 transporter in the DI differentiation medium (**Fig. 6B**). This could indicate that compounds **1**/**2** in the context of MDI-induced differentiation enhanced basal GU by upregulation of Glut1 gene expression, whereas the observed insulin-dependent GU requiring Glut4 was unrelated to an increased expression of this transporter.

Adiponectin also plays an important role in mediating GU in adipocytes and was significantly upregulated by addition of compounds **1**/**2** in the MDI protocol (**Fig. 6A**); hence, this suggests that the adipocytes might be insulin sensitive [42]. This finding fits with the stimulatory effects seen for the insulin-stimulated GU in adipocytes shown in **Fig. 4**.

We have demonstrated that a lipophilic extract of the roots of *E. purpurea* had a significant effect on basal and insulin-dependent GU and was able to activate PPARγ in transfected cell cultures. The bioassay-guided fractionation approach led to the isolation of an inseparable mixture of two new C_{12}-isomeric alkamides (compounds **1**/**2**) that significantly enhanced basal and insulin-dependent GU in adipocytes and exhibited the characteristics of PPARγ partial agonists.

Materials and Methods

Plant material

Plants of *Echinacea purpurea* (L.) Moench were propagated from seeds purchased from Rieger Hoffmann GmbH. The plantlets were raised in a greenhouse and transplanted in a sandy loam soil (Aarslev, Denmark; coordinates: 55.3° N, 10.5° E) in early June 2007. The roots were harvested in August 2010, washed and air-dried and stored at −25 °C until use. *E. purpurea* plants were authenticated by one of the authors (Dr. Kai Grevsen), and a voucher specimen (EP2010) is deposited at the Department of Food Science, Aarhus University, Denmark.

Apparatus, materials, chemicals, and reagents

Semi-preparative HPLC was performed on a Dionex UltiMate 3000 binary semipreparative LC system (Thermo Scientific), equipped with a DAD (DAD-3000 RS) and a Foxy Jr. fraction collector (Teledyne ISCO Inc.). Separations were performed on a Develosil ODS-HG-5 RP-C18 column (5 µm; 250 × 20 mm i.d., Nomura Chemical Co.). UV and MS data were collected from an HPLC-PDA-MS/MS system, LTQ XL (Linear Quadrupole 2D Ion Trap, Thermo Scientific) mass spectrometer attached to a PDA detector. HR-ESI-MS was recorded on a 10 205 micrOTOF-Q II focus high resolution mass spectrometer (Bruker Daltonics). NMR spectra were recorded on a Bruker 400 MHz spectrometer. Flash chromatography was performed in silica gel 60, particle size 0.063–0.2 mm, Merck and TLC in silica gel 60 aluminium sheets; 0.2 mm, 20 × 20 cm, Merck. MeCN, EtOAc, DCM, *n*-hexane, isopropanol, TFA, DMSO, dexamethasone, 1-methyl-3-isobutylxanthine, insulin, Oil Red O, and Rosi (HPLC purity ≥ 98 %) were purchased from Sigma-Aldrich; DMEM, FCS, CS, PBS, penicillin/streptomycin, and TRIzol reagent from Invitrogen.

Plant extraction and isolation

Fresh *E. purpurea* roots (3 kg) were homogenized and extracted twice with DCM (10 L) for 24 h in the dark at 5 °C with periodical shaking. The extracts were combined, filtered, and dried under vacuum (30 °C) to give 9.3 g crude DCM extract (yield (w/w): 0.31 %).

Initial separation of the DCM extract was done on a flash column (100 mm i.d., 300 g silica gel) conditioned with *n*-hexane. The DCM extract (8 g) was re-dissolved in DCM (20 mL), applied to the column and eluted using the following solvent gradient: 100 % *n*-hexane (600 mL), 10–90 % EtOAc in *n*-hexane in 10 % steps (600 mL each), and 100 % MeCN (1000 mL). Seventy fractions (100 mL each) were collected and combined into nine fractions (A–I) based on TLC: A (1.6 g), B (0.3 g), C (0.1 g), D (0.2 g), E (0.1 g), F (0.4 g), G (0.2 g), H (0.5 g), and I (2.9 g). TLC plates were developed using *n*-hexane-EtOAc (60 : 40) as eluent and were inspected by UV light followed by visualization with vanillin reagent. Testing of the fractions A–I in the GU bioassay revealed two active fractions, A and D (**Fig. 1A**), which were further tested in the PPARγ transactivation bioassay (**Fig. 1B**). Non-active fractions according to the GU bioassay (fraction B, C, E–I, data not shown) were not tested for PPARγ activity.

The active fractions A and D were analyzed by HPLC-PDA-APCI-MS/MS according to the method described by Thomsen et al. [14]. Fraction A was found to contain fatty acids with α-linolenic acid as a major constituent. Fraction D contained alkamides and was re-dissolved at a concentration of 10 mg/mL in MeCN and separated by semi-preparative HPLC. Mobile phase: (A) water

containing 500 ppm TFA and (B) 100% MeCN containing 500 ppm TFA. Solvent gradient: 0 min, 25% B; 55 min, 100% B; 70 min, 100% B; 85 min, 25% B; column temperature 25 °C; flow rate was 5 mL/min; injection volume was 2 mL; detection wavelengths were λ = 210, 254, and 280 nm. Separation of fraction D resulted in the isolation of dodeca-2*E*,4*E*,8*Z*,10*E*-tetraenoic acid 2-methylbutylamide (**1**) and dodeca-2*E*,4*E*,8*Z*,10*Z*-tetraenoic acid 2-methylbutylamide (**2**) as an 1 : 1 inseparable mixture (5.9 mg, HPLC purity ≥ 96%; t_R = 36.9 min) named compounds **1**/**2**, and the known metabolites dodeca-2*E*,4*E*,8*Z*-trienoic acid isobutylamide (**3**; 22.3 mg, HPLC purity ≥ 96%; t_R = 38.4 min) and dodeca-2*E*,4*E*-dienoic acid isobutylamide (**4**; 17.5 mg, HPLC purity ≥ 98%; t_R = 44.7 min). Compounds **1**/**2** were obtained as colourless oil; UV λ_{max} (nm): 235, 261. ^{1}H NMR ($CDCl_3$, 400 MHz), see ◉ **Table 1** and Supporting Information. HPLC-MS/MS (APCI; positive mode): *m/z* 262 $[M + H]^+$ (quasi-molecular precursor ion) gave the following product ions (intensities in % relative to base peak in parenthesis): *m/z* 234 (4) $[M + H - C_2H_4]^+$, 206 (3) $[M + H - C_4H_8]^+$, 192 (6) $[M + H - C_5H_{10}]^+$, 175 (28) $[M + H - C_5H_{13}N]^+$, 149 (100), 147 (24) $[M + H - C_6H_{13}NO]^+$, 133 (13), 121 (13) $[M + H - C_8H_{15}NO]^+$, 107 (18), 93 (15), 91 (6) [see also Supporting Information]. HR-ESI-MS *m/z* 262.2176 $[M(C_{17}H_{27}NO) + H]^+$ (calcd. 262.2171) [Supporting Information]. The structures of compounds **3** and **4** were established based on comparison of NMR and MS data with literature reports [12, 14, 18].

Adipocyte cell cultures

3T3-L1 preadipocytes were cultured in DMEM with 10% CS supplemented with 1% penicillin/streptomycin at 37 °C in humidified 95% air and 5% CO_2. At day two post-confluence (designated day 0), the cells were induced to differentiate with 500 µM 1-methyl-3-isobutylxanthine, 1 µM dexamethasone, and 167 nM insulin (MDI protocol), or with 1 µM dexamethasone and 167 nM insulin (DI protocol). For both protocols, the medium was replaced at day 2 with DMEM supplemented with 10% FCS, 1% penicillin/streptomycin, and 167 nM insulin and thereafter every second day with DMEM supplemented with 10% FCS and 1% penicillin/streptomycin. Extract, fractions, and pure compounds were dissolved in 0.1% (v/v) DMSO and thereafter added to the medium to a final concentration as indicated. Vehicle cells were treated with 0.1% (v/v) DMSO equal to the DMSO concentration in the medium. Mature adipocytes were treated with the compounds from days 0–8 or days 0–4 as described.

Glucose uptake in adipocytes

Mature 3T3-L1 cells were seeded in 96-well plates and differentiated according to the MDI protocol till day 8. At day 8, the cells were fed with medium supplemented with DMSO, Rosi (1 µM), and crude extract, fractions, or pure compounds. GU bioassay was performed 48 h later according to the method described by Christensen et al. [4]. GU was determined in eight parallel wells at each insulin concentration (◉ **Fig. 1 A** and **Fig. 4**; **Fig. 2S**, Supporting Information).

Peroxisome proliferator-activated receptor γ transactivation bioassay

PPARγ transactivation of vehicle [0.1% (v/v) DMSO], positive control (1 µM Rosi), crude extract, fractions, or pure compounds dissolved in DMSO (◉ **Fig. 5**) was performed on a mouse embryonic fibroblast cell line trypsinized at 70% confluence as described previously [4].

Competitive peroxisome proliferator-activated receptor γ binding assay

Competitive binding was performed using TR-FRET (LanthaScreen, Invitrogen) on Wallac EnVision (PerkinElmer). A terbium-labeled anti-GST antibody was used to label purified GST-tagged human PPARγ LBD. Energy transfer from terbium to the tracer, a fluorescent pan PPAR agonist, enabled read-out of each test compound's ability to displace the tracer. Relative fluorescence values from dose-response curves for compounds **1**/**2** and Rosi (positive control) were analysed using GraphPad Prism software (◉ **Fig. 5**). An unrestrained sigmoidal (one-binding site) dose-response curve was fitted to each data set by linear regression.

Oil Red O staining

Mature 3T3-L1 cells were differentiated according to DI or MDI protocol and treated every second day with the designated medium and DMSO, Rosi (1 µM), crude extract, fractions, or pure compounds until day 8. At day 10, cells were washed in PBS, fixed with 4% paraformaldehyde for 1 h and washed with double-distilled water. Cells were incubated with Oil Red O solution (8.57 mM Oil Red O in isopropanol) mixed 3 : 2 with water for 30 min and washed twice in water.

Molecular docking studies

Docking studies were performed using GOLD version 5.1 [43] and default parameters (GoldScore, 100% search efficiency). Protein Data Bank entry 2Q5S (human PPARγ) was selected as protein template. The active site was determined by selecting all residues within a radius of 6 Å of the co-crystalized ligand for 2Q5S. Docking was performed with a hydrogen bond to Ser342 set to constraint since this interaction has been reported to be essential for binding of PPARγ partial agonists [23]. After docking, all compounds were minimized using LigandScout's general purpose MMFF94 implementation [44]. The best docking poses for the ligands were selected by developing a 3D pharmacophore with LigandScout [45–47].

Real-time quantitative polymerase chain reaction

Total RNA was isolated on day 10 from maturing (days 0–4) 3T3-L1 adipocytes using TRIzol reagent. 500 ng of RNA were reverse transcribed with RevertAid (Fermentas) according to manufacturer's instructions. qPCR analysis was performed using the Mx3000P qPCR system (Agilent Technologies) and SYBRGreen JumpStart Taq ReadyMix (Sigma-Aldrich). Primers were purchased from Tag Copenhagen A/S. Data was analyzed using the ΔΔCt method, and gene expression was normalized to TATA box binding protein (reference gene). Primer sequences used for analysis of gene expression are shown in ◉ **Table 2**.

Statistical analysis

All data were analyzed by SAS statistical programming software (version 9.2; SAS Institute Inc.) and OriginPro software (OriginPro 8.0, OriginLab Corporation). Data were expressed as the mean ± standard deviation (SD) of three independent experiments in triplicates. The identification of significances between different groups was carried out with Student's *t*-test. A p value < 0.05 was considered statistically significant.

Supporting information

Adipocyte differentiation of DI protocol-treated 3T3-L1 preadipocytes with DMSO, 100 µg/mL DCM extract, fraction A, fraction D, 30 µM compounds **1**/**2**, and 1 µM Rosi, respectively (**Fig. 1S**), the effect of compounds **3** and **4** at a 30 µM concentration on insulin-dependent GU (**Fig. 2S**), and the HR-ESI-MS, MS/MS, ^{1}H NMR and ^{1}H–^{1}H COSY spectra of compounds **1**/**2** are available as Supporting Information.

Acknowledgements

This research was supported by the Danish Council for Strategic Research (Project No. 09–063086).

Conflict of Interest

The authors declare no conflict of interest.

Affiliations

[1] Department of Biology, University of Copenhagen, Copenhagen, Denmark
[2] Department of Chemical Engineering, Biotechnology and Environmental Technology, University of Southern Denmark, Odense, Denmark
[3] Computer-Aided Drug Design, Institute of Pharmacy, Medicinal and Pharmaceutical Chemistry, Freie Universität Berlin, Berlin, Germany
[4] Department of Food Science, Aarhus University, Aarslev, Denmark

References

1 *Barnes J, Anderson L, Gibbons S, Phillipson J. Echinacea* species (*Echinacea angustifolia* (DC.) Hell., *Echinacea pallida* (Nutt.) Nutt., *Echinacea purpurea* (L.) Moench): a review of their chemistry, pharmacology and clinical properties. J Pharm Pharmacol 2005; 57: 929–954
2 *Woelkart K, Bauer R.* The role of alkamides as an active principle of *Echinacea*. Planta Med 2007; 73: 615–623
3 *Christensen KB, Minet A, Svenstrup H, Grevsen K, Zhang H, Schrader E, Rimbach G, Wein S, Wolfram S, Kristiansen K, Christensen LP.* Identification of plant extracts with potential antidiabetic properties: effect on human peroxisome proliferator-activated receptor (PPAR), adipocyte differentiation and insulin-stimulated glucose uptake. Phytother Res 2009; 23: 1316–1325
4 *Christensen KB, Petersen RK, Petersen S, Kristiansen K, Christensen LP.* Activation of PPARγ by metabolites from the flowers of purple coneflower (*Echinacea purpurea*). J Nat Prod 2009; 72: 933–937
5 *Nawrocki AR, Scherer PE.* Keynote review: the adipocyte as a drug discovery target. Drug Discov Today 2005; 10: 1219–1230
6 *Rosen ED, Spiegelman BM.* Molecular regulation of adipogenesis. Annu Rev Cell Dev Biol 2000; 16: 145–171
7 *Cariou B, Charbonnel B, Staels B.* Thiazolidinediones and PPARγ agonists: time for a reassessment. Trends Endocrinol Metab 2012; 23: 205–215
8 *Yeh GY, Eisenberg DM, Kaptchnuk TJ, Phillips RS.* Systematic review of herbs and dietary supplements for glycemic control in diabetes. Diabetes Care 2013; 26: 1277–1294
9 *Starvaggi Cucuzza L, Motta M, Accornero P, Baratta M.* Effect of *Echinacea augustifolia* extract on cell viability and differentiation in mammary epithelial cells. Phytomed 2008; 15: 555–562
10 *Spelman K, Liams-Hauser K, Cech NB, Taylor EW, Smirnoff N, Wenner CA.* Role of PPARγ in IL-2 inhibition in T cells by *Echinacea*-derived undeca-2*E*-ene-8, 10-diynoic acid isobutylamide. Int Immunopharmacol 2009; 9: 1260–1264
11 *Goey AKL, Rosing H, Meijerman I, Sparidans RW, Schellens JHM, Beijnen JH.* The bioanalysis of the major *Echinacea purpurea* constituents dodeca-2*E*,4*E*,8*Z*,10*E*/*Z*-tetraenoic acid isobutylamides in human plasma using LC-MS/MS. J Chromatogr B 2012; 902: 151–156
12 *Bauer R, Remiger P, Wagner H.* Alkamides from the roots of *Echinacea purpurea*. Phytochem 1988; 27: 2339–2342
13 *Spelman K, Wetschler MH, Cech NB.* Comparison of alkylamide yield in ethanolic extracts prepared from fresh versus dry *Echinacea purpurea* utilizing HPLC-ESI-MS. J Pharm Biomed Anal 2009; 49: 1141–1149
14 *Thomsen MO, Fretté XC, Christensen KB, Christensen LP, Grevsen K.* Seasonal variations in the concentrations of lipophilic compounds and phenolic acids in the roots of *Echinacea purpurea* and *Echinacea pallida*. J Agric Food Chem 2012; 60: 12131–12141
15 *Takahara Y, Kobayashi T, Takemoto K, Adachi T, Osaki K, Kawahara K, Tsujimoto G.* Pharmacogenomics of cardiovascular pharmacology: development of an informatics system for analysis of DNA microarray data with focus on lipid metabolism. J Pharmacol Sci 2008; 107: 1–7
16 *Ghafoorunissa, Ibrahim A, Natarajan S.* Substituting dietary linoleic acid with α-linolenic acid improves insulin sensitivity in sucrose fed rats. Biochim Biophys Acta 2005; 21: 67–75
17 *Poudyal H, Panchal SK, Ward LC, Brown L.* Effects of ALA, EPA and DHA in high-carbohydrate, high-fat diet-induced metabolic syndrome in rats. J Nutr Biochem 2013; 24: 1041–1052
18 *Bauer R, Remiger P.* TLC and HPLC analysis of alkamides in *Echinacea* drugs. Planta Med 1989; 55: 367–371
19 *Cech NB, Eleazer MS, Shoffner LT, Crosswhite MR, Davis AC, Mortenson AM.* High performance liquid chromatography/electrospray ionization mass spectrometry for simultaneous analysis of alkamides and caffeic acid derivatives from *Echinacea purpurea* extracts. J Chromatogr A 2006; 1103: 219–228
20 *Mudge E, Loes-Lutz D, Brown P, Scheiber A.* Analysis of alkylamides in *Echinacea purpurea* materials and dietary supplements by ultrafast liquid chromatography with diode array and mass spectrometric detection. J Agric Food Chem 2011; 59: 8086–8094
21 *Pellati F, Epifano F, Contaldo N, Orlandini G, Cavicchi L, Genovese S, Bertelli D, Bevenuti S, Curini M, Bertaccini A, Bellardi MG.* Chromatographic methods for metabolite profiling of virus- and phytoplasma-infected plants of *Echinacea purpurea*. J Agric Food Chem 2011; 59: 10425–10434
22 *Nakatani N, Nagashima M.* Pungent alkamides from *Spilanthes acmella* L. var. *oleracae* Clarke. Biosci Biotechnol Biochem 1992; 56: 759–762
23 *Atanasov AG, Wang JN, Gu SP, Bu J, Kramer MP, Baumgartner L, Fakhrudin N, Ladurner A, Malainer C, Vuorinen A, Noha SM, Schwaiger S, Rollinger JM, Schuster D, Stuppner H, Dirsch VM, Heiss EH.* Honokiol: A non-adipogenic PPARγ agonist from nature. Biochim Biophys Acta 2013; 1830: 4813–4819
24 *Guasch L, Sala E, Valls C, Blay M, Mulero M, Arola L, Pujadas G, Garcia-Vallvé S.* Structural insights for the design of new PPARgamma partial agonists with high binding affinity and low transactivation activity. J Comput Aided Mol Des 2011; 25: 717–728
25 *Zoete V, Grosdidier A, Michielin O.* Peroxisome proliferator-activated receptor structures: ligand specificity, molecular switch and interactions with regulators. Biochim Biophys Acta 2007; 1771: 915–925
26 *Berger JP, Petro AE, Macnaul KL, Kelly LJ, Zhang BB, Richards K, Elbrecht A, Johnson BA, Zhou G, Doebber TW, Biswas C, Parikh M, Sharma N, Tanen MR, Thompson GM, Ventre J, Adams AD, Mosley R, Surwit RS, Moller DE.* Distinct properties and advantages of a novel peroxisome proliferator-activated protein γ selective modulator. Mol Endocrinol 2003; 17: 662–676
27 *Thoennes SR, Tate PL, Price TM, Kilgore MW.* Differential transcriptional activation of peroxisome proliferator-activated receptor gamma by omega-3 and omega-6 fatty acids in MCF-7 cells. Mol Cell Endocrinol 2000; 160: 67–73
28 *Desvergne B, Wahli W.* Peroxisome proliferator-activated receptors: nuclear control of metabolism. Endocr Rev 1999; 20: 649–688
29 *Dussault I, Forman BM.* Prostaglandins and fatty acids regulate transcriptional signaling via the peroxisome proliferator activated receptor nuclear receptors. Prostaglandins Other Lipid Mediat 2000; 62: 1–13
30 *Hammond VJ, Morgan AH, Lauder S, Thomas CP, Brown S, Freeman BA, Lloyd CM, Davies J, Bush A, Levonen AL, Kansanen E, Villacorta L, Chen YE, Porter N, Garcia-Diaz YM, Schopfer FJ, O'Donnell VB.* Novel ketophospholipids are generated by monocytes and macrophages, detected in cystic fibrosis, and activate peroxisome proliferator-activated receptor-γ. J Biol Chem 2012; 287: 41651–41666
31 *Atanasov AG, Blunder M, Fakhrudin N, Liu X, Noha SM, Malainer C, Kramer MP, Cocic A, Kunert O, Schinkovitz A, Heiss EH, Schuster D, Dirsch VM, Bauer R.* Polyacetylenes from *Notopterygium incisum* – new selective partial agonists of peroxisome proliferator-activated receptor-gamma. PLoS ONE 2013; 8: e61755
32 *Waku T, Shiraki T, Oyama T, Fujimoto Y, Maebara K, Kamiya N, Jingami H, Morikawa K.* Structural insight into PPARγ activation through covalent modification with endogenous fatty acids. J Mol Biol 2009; 385: 188–199

33 *Itoh T, Fairall L, Amin K, Inaba Y, Szanto A, Balint BL, Nagy L, Yamamoto K, Schwabe JWR.* Structural basis for the activation of PPARγ by oxidized fatty acids. Nat Struct Mol Biol 2008; 15: 924–931

34 *Shiraki T, Kamiya N, Shiki S, Kodama TS, Kakizuka A, Jingami H.* α,β-Unsaturated ketone is a core moiety of natural ligands for covalent binding to peroxisome proliferator-activated receptor γ. J Biol Chem 2005; 280: 14145–14153

35 *McLaughlin T, Sherman A, Tsao P, Gonzalez O, Yee G, Lamendola C, Reaven GM, Cushman SW.* Enhanced proportion of small adipose cells in insulin-resistant vs. insulin-sensitive obese individuals implicates impaired adipogenesis. Diabetologia 2007; 50: 1707–1715

36 *Hallenborg P, Jorgensen C, Petersen RK, Feddersen S, Araujo P, Markt P, Langer T, Furstenberger G, Krieg P, Koppen A, Kalkhoven E, Madsen L, Kristiansen K.* Epidermis-type lipoxygenase 3 regulates adipocyte differentiation and peroxisome proliferator-activated receptor gamma activity. Mol Cell Biol 2010; 16: 4077–4091

37 *Spiegelman BM.* PPAR-gamma: adipogenic regulator and thiazolidinedione receptor. Diabetes 1998; 47: 507–514

38 *Ribon V, Johnson JH, Camp HS, Saltiel AR.* Thiazolidinediones and insulin resistance: peroxisome proliferator activated receptor γ activation stimulates expression of CAP gene. Proc Natl Acad Sci USA 1998; 95: 14751–14756

39 *Wood IS, Trayhurn P.* Glucose transporter (GLUT and SGLT): expanded families of sugar transport proteins. Br J Nutr 2003; 89: 3–9

40 *Gregoire FM, Johnson PR, Greenwood MR.* Comparison of the adipoconversion of preadipocytes derived from lean and obese Zucker rats in serum-free cultures. Int J Obes Relat Metab Disord 1995; 19: 664–670

41 *Shang W, Yang Y, Jiang B, Jin H, Zhou L, Liu S, Chen M.* Ginsenoside Rb1 promotes adipogenesis in 3T3-L1 cells by enhacing PPARγ2 and C/EBPα gene expression. Life Sci 2007; 80: 618–625

42 *Yamauchi T, Kamon J, Waki H, Terauchi Y, Kubota N, Hara K, Mori Y, Ide T, Murakami K, Tsuboyama-Kasaoka N, Ezaki O, Akanuma Y, Gavrilova O, Vinson C, Reitman ML, Kagechika H, Shudo K, Yoda M, Nakano Y, Tobe K, Nagai R, Kimura S, Tomita M, Froguel P, Kadowaki T.* The fat-derived hormone adiponectin reverses insulin resistance associated with both lipoatrophy and obesity. Nat Med 2001; 7: 941–946

43 *Jones G, Willett P, Glen RC.* Molecular recognition of receptor sites using a genetic algorithm with a description of desolvation. J Mol Biol 1995; 245: 43–53

44 *Halgren TA.* Merck molecular force field. I. Basis, form, scope, parameterization, and performance of MMFF94. J Comput Chem 1996; 17: 490–519

45 *Seidel T, Ibis G, Bendix F, Wolber G.* Strategies for 3D pharmacophore-based virtual screening. Drug Discov Today Technol 2010; 7: 221–228

46 *Wolber G, Dornhofer AA, Langer T.* Efficient overlay of small organic molecules using 3D pharmacophores. J Comput Aided Mol Des 2006; 20: 773–788

47 *Wolber G, Langer T.* LigandScout: 3-D pharmacophores derived from protein-bound ligands and their use as virtual screening filters. J Chem Inform Model 2005; 45: 160–169